

# Insights into Gravitinos Abundance, Cosmic Strings and Stochastic Gravitational Wave Background

K. El Bourakadi<sup>1,2,\*</sup>, G. Otalora<sup>1,†</sup>, A. Burton-Villalobos<sup>1,‡</sup>, H. Chakir<sup>2,§</sup>, M. Ferricha-Alami<sup>3,¶</sup> and M. Bennai<sup>3,\*\*</sup>

<sup>1</sup>*Departamento de Física, Facultad de Ciencias,  
Universidad de Tarapacá, Casilla 7-D, Arica, Chile.*

<sup>2</sup>*Subatomic Research and Applications Team,  
Faculty of Science Ben M'sik,  
Casablanca Hassan II University, Morocco  
and*

<sup>3</sup>*Quantum Physics and Magnetism Team, LPMC,  
Faculty of Science Ben M'sik,  
Casablanca Hassan II University, Morocco.*

In this paper, we investigate D-term inflation within the framework of supergravity, employing the minimal Kähler potential. Our study reveals that this model can overcome the  $\eta$ -problem found in F-term models. Additionally, we explore reheating dynamics and gravitino production, emphasizing the interplay between reheating temperature, spectral index, and gravitino abundance. Our analysis indicates that gravitino production is sensitive to the equation of state during reheating, affecting the reheating temperature and subsequent dark matter relic density. Perturbation theory reveals that Primordial Gravitational Waves (PGWs) evolve according to second-order effects arising from first-order curvature perturbations. In fact, the spectral energy density of these waves is particularly relevant to Pulsar Timing Array (PTA) observations. Furthermore, we analyze gravitational waves generated by cosmic strings, providing critical constraints on early Universe dynamics and cosmic string properties. The dimensionless string tension significantly influences the stochastic gravitational wave background (SGWB) produced by cosmic strings post-inflation. Finally, the SGWB produced by cosmic strings is influenced by the energy scales of inflation and string formation.

## I. INTRODUCTION

Supersymmetric (SUSY) inflation [1–4] provides an appealing framework for connecting inflation with particle physics models rooted in grand unified theories (GUTs) [5]. In the simplest models, the soft supersymmetry breaking terms are crucial for aligning predictions of the scalar spectral index with cosmic microwave background (CMB) observations [6],[7]. SUSY provides an appealing solution to the analogous hierarchy problem in the Standard Model (SM) of particle physics and also facilitates the unification of the three gauge couplings. Notably, the local version of supersymmetry — supergravity (SUGRA) — would dominate the dynamics of the early Universe when high-energy physics played a crucial role. Therefore, considering inflation within the framework of supergravity is quite natural. However, integrating inflation into supergravity is a challenging task. This difficulty arises mainly because the SUSY breaking potential term, essential for inflation, typically imparts an additional mass to the would-be inflaton, thereby disrupting the flatness of the inflaton potential [8, 9]. To achieve successful inflation that aligns with observational data from large-scale structures and the anisotropy of CMB radiation, the potential of the scalar field, known as the inflaton, must be very flat. This required flatness of the potential can be achieved through the mechanisms provided by supersymmetry or supergravity. In supersymmetric models, the scalar potential is composed of contributions from both the F-term and D-term.

Specifically, in F-term inflation models, where the vacuum energy that drives the inflationary expansion predominantly comes from the F-term, the inflaton mass is generally on the same order as the Hubble parameter  $H$  during inflation [10]. Consequently, achieving a sufficiently long expansion to address the horizon and flatness problems is challenging. This issue is referred to as the eta problem in inflation models within the framework of supergravity. Conversely, D-term inflation, in which the vacuum energy is supplied by the D-term, does not encounter this problem [11, 12]. Therefore, from this perspective, D-term inflation is more appealing than F-term inflation. However, it has

\* k.elbourakadi@yahoo.com

† giovanni.otalora@academicos.uta.cl

‡ andres.burton.villalobos@alumnos.uta.cl

§ chakir10@gmail.com

¶ ferrichaalami@yahoo.fr

\*\* mdbennai@yahoo.fr

been discovered that the D-term inflation model also has its own set of issues [13]. For instance, from an observational standpoint, cosmic strings generated after inflation can significantly impact the spectrum of CMB anisotropy [14], as this model is a type of hybrid inflation. Additionally, there are concerns about the validity of the D-term inflation potential, since the inflaton requires a large initial value on the order of the (sub-)Planck scale for a natural model parameter [15]. Therefore, D-term inflation appears to be under considerable scrutiny. Additionally, within the framework of (heterotic) string models, there are two further issues: the runaway behavior of the dilaton and an excessively large magnitude of the Fayet-Iliopoulos (FI) term [16].

Given the current and anticipated future constraints on inflaton decay via CMB limits on  $N_{re}$  and the competition with constraints from gravitino abundance in supersymmetric models, we revisit the issue of gravitino production following inflation. A well-understood source of gravitinos is their production through particle collisions in the thermal plasma that fills the Universe after reheating [17–19]. However, gravitinos could also have been produced by particle collisions before the reheating process was complete, either from collisions of relativistic inflaton decay products before thermalization or within any dilute thermal plasma formed by these collisions while inflaton decay was still ongoing [20].

Cosmic strings are intriguing messengers from the early Universe due to their distinctive signatures in the stochastic gravitational wave background (SGWB). Recent NANOGrav 12.5-year data has provided evidence of a stochastic process at nanohertz frequencies, which has been interpreted as SGWB in numerous recent studies [21–24]. Relic gravitational waves (GWs) offer a fascinating window into the exploration of early Universe cosmology [25]. Cosmic strings generate powerful bursts of gravitational radiation that could be detected by interferometric gravitational wave detectors such as LIGO, Virgo, and LISA [26, 27]. Additionally, the SGWB can be detected or constrained through various observations, including big bang nucleosynthesis (BBN), pulsar timing experiments, and interferometric gravitational wave detectors [28].

The paper is organized as follows, in Sec. II we examine supergravity formalism, in Sec. III we focus on the D-term model for the case of the minimal Kähler potential. In Sec. IV, we apply the previous findings in the study of the reheating process and its relation to gravitinos production. In Sec. V, we link the primordial gravitational waves production from different epochs in the light of the chosen supergravity formalism, which is constrained by PTA observations. In Sec. VI, we study the gravitational waves production due to networks of cosmic strings. In Sec. VII, we conclude.

## II. SUPERGRAVITY FORMALISM

The supergravity lagrangian scalar part can be defined by the superpotential  $W(\Theta_i)$ , Kähler potential  $K(\Theta_i, \Theta_i^*)$ , and gauge kinetic function  $f(\Theta_i)$  [29–31].  $W$  and  $f$  are holomorphic functions of complex scalar fields, whereas the initial function  $K$  is non-holomorphic and operates as a real function of the scalar fields  $\Theta_i$  and their conjugates  $\Theta_i^*$ . The three functions mentioned above are initially defined in terms of (chiral) superfields. Since our primary focus is on the scalar component of a superfield, we equate a superfield with its complex scalar counterpart, denoting both by the same symbol. The action of the complex scalar fields, when minimally coupled to gravity, comprises both kinetic and potential components.

$$S = \int d^4x \sqrt{-g} \left[ \frac{1}{\sqrt{-g}} \mathcal{L}_{kin} - V(\Theta_i, \Theta_i^*) \right]. \quad (2.1)$$

The kinetic terms of the scalar fields are dictated by the Kähler potential, denoted as  $K$ , and expressed as follows:

$$\frac{1}{\sqrt{-g}} \mathcal{L}_{kin} = -K_{ij^*} D_\mu \Theta_i D_\nu \Theta_j^* g^{\mu\nu}, \quad (2.2)$$

with  $K_{ij^*} = \partial^2 K / \partial \Theta_i \partial \Theta_j^*$ , and  $D_\mu$  denotes the covariant derivative in the gauge field context. The potential  $V$  for scalar fields  $\Theta_i$  consists of two components, namely, the F-term  $V_F$  and the D-term  $V_D$ . Here the F-term component which is determined by both the superpotential  $W$  and the Kähler potential  $K$  is given by,

$$V_F = e^K \left[ D_{\Theta_i} W K_{ij^*}^{-1} D_{\Theta_j^*} W^* - \frac{3|W|^2}{M_p^2} \right], \quad (2.3)$$

where

$$D_{\Theta_i} W = \frac{\partial W}{\partial \Theta_i} + \frac{1}{M_p^2} \frac{\partial K}{\partial \Theta_i} W. \quad (2.4)$$

Conversely, the D-term  $V_D$  is associated with gauge symmetry and is defined by the gauge kinetic function and the Kähler potential,

$$V_D = \frac{1}{2} \sum [Re f_{ab}(\Theta_i)]^{-1} g_a g_b D_a D_b, \quad (2.5)$$

where

$$D_a = \Theta_i (T_a)_j^i \frac{\partial K}{\partial \Theta_i} + \xi_a. \quad (2.6)$$

In this context, the subscripts ( $a$ ) and ( $b$ ) denote gauge symmetries, where  $g_a$  represents the gauge coupling constant, and  $T_a$  stands for the corresponding generator. The term  $\xi_a$  is referred to as the Fayet–Iliopoulos (*FI*) term, which is non-zero exclusively when the gauge symmetry is Abelian, specifically  $U(1)$  symmetry. Keep in mind that within a supersymmetric framework, the tree-level potential during inflation comprises both an F-term and a D-term. These two components exhibit distinct characteristics, and in the context of all inflationary models, it is noteworthy that dominance is typically attributed to only one of these terms.

In certain models rooted in Supergravity, such as the one under consideration here with a nonminimal Kähler potential, the exponential term  $e^K$  contributes a term  $V$  to the effective mass squared, roughly of the order of  $H^2$  (the Hubble scale squared), affecting all scalar fields. Consequently, inflation experiences an effective mass squared  $V_g = \sum \left| \frac{\partial W}{\partial \Theta_i} \right|^2 = 3H^2$  [32], introducing a contribution to the slow-roll parameter  $\eta$ . This contribution results in a violation of the slow-roll conditions ( $|\eta| \ll 1$ ) and leads to the so-called  $\eta$ -problem

$$\eta = M_p^2 \frac{V''}{V} \simeq \frac{1}{3} \left( \frac{m}{H} \right)^2 \simeq 1.$$

Addressing this challenge has prompted the proposal of various approaches. Here, we are only interested in the use of D-term hybrid inflation, which can provide positive energy in D-term potential. This allows for the realization of inflation while avoiding the  $\eta$ -problem.

### III. D-TERM HYBRID MODEL

Constructing an inflation model in supergravity faces a significant challenge arising from the F-term, particularly the exponential factor associated with it. Hence, achieving a positive potential energy in the D-term could pave the way for successful inflation without encountering the  $\eta$  problem. This insight was initially highlighted in Ref. [33].

Let us consider a D-term model of hybrid inflation as introduced in [34, 35],

$$W = \lambda S \Theta_+ \Theta_-, \quad (3.1)$$

where  $\lambda$  is the coupling constant, and  $S$ ,  $\Theta_+$ , and  $\Theta_-$  are three (chiral) superfields. The superpotential remains unchanged under a  $U(1)$  gauge symmetry, with assigned charges of 0, +1, and -1 for the fields  $S$ ,  $\Theta_+$ , and  $\Theta_-$ , respectively. Additionally, it exhibits an  $R$  symmetry governing the transformation of these fields as follows:

$$S(\theta) \rightarrow e^{2i\alpha} S(\theta e^{i\alpha}), \quad \Theta_+ \Theta_-(\theta) \rightarrow \Theta_+ \Theta_-(\theta e^{i\alpha}), \quad (3.2)$$

and considering the minimal Kähler potential,

$$K = |S|^2 + |\Theta_+|^2 + |\Theta_-|^2. \quad (3.3)$$

From Eqs. (2.3) and (2.5) the tree level scalar potential is given by,

$$V(S, \Theta_+, \Theta_-) = \lambda^2 e^{|S|^2 + |\Theta_+|^2 + |\Theta_-|^2} \left[ |\Theta_+ \Theta_-|^2 + |S \Theta_-|^2 + |S \Theta_+|^2 + \left( |S|^2 + |\Theta_+|^2 + |\Theta_-|^2 + 3 \right) |S \Theta_+ \Theta_-|^2 \right] + \frac{g^2}{2} \left( |\Theta_+|^2 - |\Theta_-|^2 + \xi \right). \quad (3.4)$$

Here,  $g$  represents the gauge coupling constant,  $\xi$  is a non-zero FI term, and we have adopted a minimal gauge kinetic function. This potential exhibits a distinctive global minimum  $V = 0$  at  $S = \Theta_+ = 0, \Theta_- = \sqrt{\xi}$ . Yet, when  $|S|$  is significantly large, the potential displays a local minimum with a positive energy density at  $\Theta_+ = \Theta_- = 0$ . To

determine the critical value  $S_c$  of  $|S|$ , we compute the mass matrix of  $\Theta_+$  and  $\Theta_-$  along the inflationary trajectory where  $\Theta_+ = \Theta_- = 0$ . This is expressed as:

$$V_{mass} = m_+^2 |\Theta_+|^2 + m_-^2 |\Theta_-|^2, \quad (3.5)$$

with

$$m_+^2 = \lambda^2 |S|^2 e^{|S|^2} + g^2 \xi, \quad m_-^2 = \lambda^2 |S|^2 e^{|S|^2} - g^2 \xi. \quad (3.6)$$

Hence, provided that  $m_-^2 \geq 0$ , corresponding to  $|S| \geq S_c \simeq g\sqrt{\xi}/\lambda$  for  $S_c \lesssim 1$ , the local minimum at  $\Theta_+ = \Theta_- = 0$  remains stable, leading to inflation driven by the positive potential energy density of  $g^2 \xi^2/2$ . Moreover, this mass split induces quantum corrections computed using the standard formula [32, 36],

$$V_{1L} = \frac{1}{32\pi^2} \left[ m_+^4 \ln \left( \frac{\lambda^2 |S|^2 e^{|S|^2} + g^2 \xi}{\Lambda^2} \right) + m_-^4 \ln \left( \frac{\lambda^2 |S|^2 e^{|S|^2} + g^2 \xi}{\Lambda^2} \right) - 2\lambda^4 |S|^4 e^{|S|^2} \ln \left( \frac{\lambda^2 |S|^2 e^{|S|^2}}{\Lambda^2} \right) \right], \quad (3.7)$$

and when  $|S| \gg S_c$ , the effective potential of  $S$  during inflation is approximated as,

$$V(S) \simeq \frac{g^2 \xi^2}{2} \left[ 1 + \frac{g^2}{8\pi^2} \ln \left( \frac{\lambda^2 |S|^2 e^{|S|^2}}{\Lambda^2} \right) \right]. \quad (3.8)$$

Given that the potential is independent of the phase of the complex scalar field  $S$ , we can propose its real part as  $\sigma \equiv \sqrt{2} \text{Re} S$ . Subsequently, for  $\sigma_c \ll \sigma \lesssim 1$ , the effective potential of the inflaton field  $\sigma$  is expressed as:

$$V(\sigma) \simeq \frac{g^2 \xi^2}{2} \left[ 1 + \frac{g^2}{8\pi^2} \ln \left( \frac{\lambda^2 \sigma^2}{2\Lambda^2} \right) \right]. \quad (3.9)$$

During the inflationary period, the slow roll parameters take the form

$$\epsilon \simeq \frac{g^4}{32\pi^4 \sigma^2}, \quad (3.10)$$

$$\eta \simeq -\frac{g^2}{4\pi^2 \sigma^2}, \quad (3.11)$$

and the e-folding number  $N$  is estimated as

$$N \simeq \frac{2\pi^2}{g^2} (\sigma_k^2 - \sigma_{end}^2). \quad (3.12)$$

Throughout the inflationary regime, curvature perturbations arose from inflaton fluctuations. The amplitude of these perturbations in the comoving gauge  $\mathcal{R}$  [37–41], measured on the comoving scale of  $2\pi/k$ , is determined as,

$$\mathcal{R}^2 \simeq \frac{1}{24\pi^2} \frac{V}{\epsilon} = \frac{N}{3} \xi^2. \quad (3.13)$$

Here,  $k$  represents the epoch when the  $k$  mode exited the Hubble radius in the course of inflation, as indicated in [42, 43, 46]. Conversely, gravitational wave tensor perturbations  $h$  are also generated, and their amplitude on the comoving scale of  $2\pi/k$  is specified in Ref. [47], and calculated in this model as,

$$h_k^2 \simeq \frac{2}{3\pi^2} V(\sigma_k) = \frac{g^2 \xi^2}{3\pi^2}. \quad (3.14)$$

Then, the tensor-to-scalar ratio  $r$  is given by

$$r \equiv \frac{h_k^2}{\mathcal{R}^2} \simeq 16\epsilon \quad (3.15)$$

where  $h_k^2 = 2H_k^2/\pi^2$ , and for a chosen pivot scale, the power spectrum of scalar perturbation can be considered as  $\mathcal{R}^2 \simeq A_s$ .

#### IV. REHEATING DYNAMICS AND GRAVITINOS PRODUCTION

In the initial stages, the quasi-de-Sitter phase is driven by the inflaton field, resulting in  $N_k$  e-folds of expansion. The comoving horizon scale decreases proportionally to  $\sim a^{-1}$  during this period. Following the conclusion of accelerated expansion and the subsequent expansion of the comoving horizon, the reheating phase begins [44]. After an additional  $N_{re}$  e-folds of expansion, all the energy stored in the inflaton field is completely dissipated, leading to the formation of a hot plasma with a reheating temperature of  $T_{re}$ . Following this phase, the Universe undergoes  $N_{RD}$  e-folds of expansion in a state of radiation domination before transitioning into a state of matter domination.

In cosmology, we observe perturbation modes that exhibit magnitudes comparable to the size of the cosmic horizon. For instance, Planck identifies the pivot scale at  $k = 0.05 Mpc^{-1}$  [45]. The comoving Hubble scale, denoted as  $a_k H_k = k$  is associated with the current timescale in relation to the moment when this particular mode crossed the horizon [48, 49],

$$\frac{k}{a_0 H_0} = \frac{a_k}{a_{end}} \frac{a_{end}}{a_{re}} \frac{a_{re}}{a_{eq}} \frac{a_{eq} H_{eq}}{a_0 H_0} \frac{H_k}{H_{eq}}. \quad (4.1)$$

Quantities represented by a subscript ( $k$ ) are calculated at the point of horizon exit. Other subscripts denote various epochs, including the end of inflation ( $_{end}$ ), reheating ( $_{re}$ ), radiation-matter equality ( $_{eq}$ ), and the present time ( $_0$ ). It is noteworthy that  $\ln\left(\frac{a_k}{a_{end}}\right) = N_k$ ,  $\ln\left(\frac{a_{end}}{a_{re}}\right) = N_{re}$  and  $\ln\left(\frac{a_{re}}{a_{eq}}\right) = N_{RD}$ .

A connection between the temperature at the end of reheating  $T_{re}$  and the CMB temperature  $T_0$  can be established by considering factors is given by,

$$T_{re} = \left(\frac{43}{11g_{re}}\right)^{\frac{1}{3}} \left(\frac{a_0 T_0}{k}\right) H_k e^{-N_k} e^{-N_{re}}. \quad (4.2)$$

On the other hand, the reheating duration can be expressed as,

$$N_{re} = \frac{1}{3(1+\omega_{re})} \ln\left(\frac{30 \cdot \frac{3}{2} V_{end}}{\pi^2 g_{re} T_{re}^4}\right), \quad (4.3)$$

and thus, the final form of reheating temperature is described as a function of the number of inflationary e-foldings  $N_k$ , the Hubble parameter  $H_k$  and the potential value at the end of inflation  $V_{end}$  as [43, 46, 50],

$$T_{re} = \left[ \left(\frac{43}{11g_{re}}\right)^{\frac{1}{3}} \frac{a_0 T_0}{k} H_k e^{-N_k} \left[\frac{3^2 \cdot 5 V_{end}}{\pi^2 g_{re}}\right]^{-\frac{1}{3(1+\omega_{re})}} \right]^{\frac{3(1+\omega_{re})}{3\omega_{re}-1}}. \quad (4.4)$$

To determine the reheating temperature,  $T_{re}$ , for a specific model, one must calculate  $N_k$ ,  $H_k$ ,  $V_{end}$ , and the potential at the end of inflation by using the formula  $V_{end} = V(\sigma_{end})$ , and knowing that  $\sigma_{end}$  is determined considering  $|\eta| = 1$ .

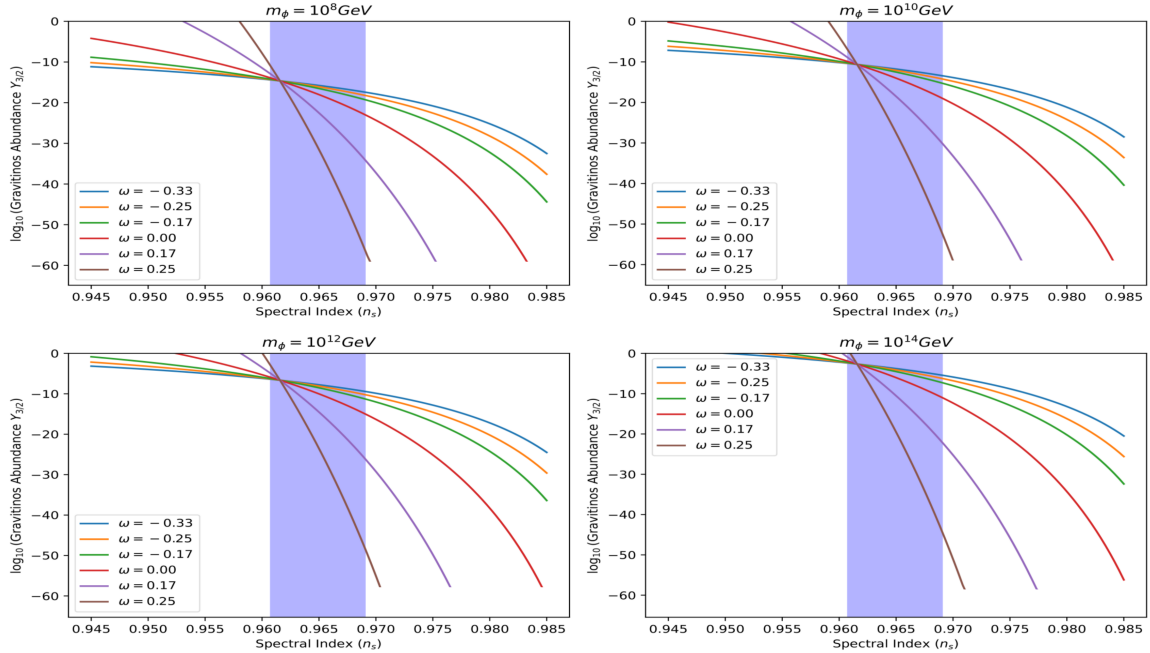
The SUGRA effects result in the coupling of the inflaton field  $\phi$  to all matter fields, provided there is a non-zero vacuum expectation value (VEV). The interactions with fermions are appropriately expressed in the context of the total Kähler potential, denoted as  $G = K + \ln|W|^2$ , and such that:

$$\mathcal{L} = -\frac{1}{2} e^{G/2} G_{\phi i j k} \phi \psi^i \psi^j \varphi^k + h.c. \quad (4.5)$$

In the given context,  $\varphi^i$  represents a scalar field, and  $\psi^i$  represents a fermion in a 2-spinor representation. We make the assumption that  $G_i$  is much smaller than  $\mathcal{O}(1)$  for all fields, excluding the field responsible for SUSY breaking. The presence of the SUSY breaking field may lead to the suppression of the contribution proportional to  $G_\phi$  during the inflaton decay due to interference [51, 52]. In this section, we simplify our analysis by assuming the minimal Kähler potential. Consequently, the Kähler potential lacks non-renormalizable terms. Despite isolating the inflaton field from other fields in the global SUSY Lagrangian, the presence of (SUGRA) corrections enables its decay. The coupling constants are expanded at the vacuum state [53].

$$G_{\phi i j k} = -\frac{W_\phi}{W} \frac{W_{ijk}}{W} + \frac{W_{\phi i j k}}{W} \simeq K_\phi \frac{W_{ijk}}{W} + \frac{W_{\phi i j k}}{W}. \quad (4.6)$$

In previous analysis [53], the assumption was made that the Vacuum Expectation Values (VEVs) are effectively negligible for all fields except the inflaton. We employed the condition  $G_\phi \ll \langle \phi \rangle$  in the final equation. Notably, we

Gravitino Abundance as a Function of Spectral Index for Different  $m_\phi$  ValuesFIG. 1. The gravitino abundance  $Y_{3/2}$  as functions of the spectral index  $n_s$  for different values of the equation of state  $\omega$ .

observed that the outcome remains invariant under Kähler transformation, and these constants tend to zero in the global SUSY limit. Subsequently, the decay rates are computed

$$\Gamma_{3/2}(\phi \rightarrow \psi^i \psi^j \varphi^k) \simeq \frac{N_f}{1536\pi^3} |Y_{ijk}|^2 \left(\frac{\langle\phi\rangle}{M_p}\right)^2 \frac{m_\phi^3}{M_p^2}, \quad (4.7)$$

Here,  $N_f$  represents the count of final states, and the Yukawa coupling  $Y_{ijk}$  is denoted as  $W_{ijk}$ . In this context, we have disregarded the masses of the particles in the final state and employed  $K = \varphi^\dagger \varphi$  for the inflaton. Additionally, it is assumed here that the particles  $\psi^i$  and  $\psi^j$  are non-identical. The decay rates of the inflaton into scalar particles align with the previously mentioned results. Indeed, considering the scalar potential,  $V = e^G (G^j G_j - 3)$ , the estimated decay amplitude of  $\phi^* \Rightarrow \varphi^i \varphi^j \varphi^k$  is denoted as  $V_{\bar{\phi}ijk}$ . Given the sizable SUSY mass of the inflaton, this amplitude is approximately proportional to  $e^{G/2} G_{\phi_{ijk}}$ , multiplied by the inflaton mass,  $m_\phi \simeq e^{G/2} |G_\phi^\phi|$ . The inflaton's decay into a pair of gravitinos occurs at the rate  $\Gamma$ . The resulting gravitino abundance  $Y_{3/2}$  is then calculated, with  $Y_{3/2}$  equal to the ratio of the final gravitino abundance to the entropy density  $\frac{n_{3/2}}{s}$  [54–56].

$$Y_{3/2} \simeq 2 \times 10^{-11} \left(\frac{10^6 \text{ GeV}}{T_{re}}\right) \left(\frac{m_\phi \times \langle\phi\rangle}{10^{27} \text{ GeV}^2}\right)^2. \quad (4.8)$$

The plot in Fig. 1 displays the gravitino abundance  $Y_{3/2}$  as a function of the spectral index  $n_s$  for different values of the inflaton mass  $m_\phi$ . Each subplot corresponds to a specific  $m_\phi$  values, ranging from  $10^8 \text{ GeV}$  to  $10^{14} \text{ GeV}$ . Different curves representing various equation of state parameter values during reheating  $\omega$ , with a shaded region highlighting the Planck bound on  $n_s = 0.9649 \pm 0.0042$  according to recent observations [57].

From the given formalism, the abundance of gravitinos produced during the reheating phase, denoted as  $Y_{3/2}$  is significantly dependent on the reheating temperature  $T_{re}$ , which is affected by  $\omega$ . The curves of the gravitinos abundance tend towards the central value where all the lines with the different equation of state values converge. This central value of the abundance curves corresponds to the highest reheating temperature, and all the lines coincide within the observed bound on the spectral index  $n_s$ . Higher  $m_\phi$  values generally lead to increased gravitino production when considering the maximum reheating temperature, while different  $\omega$  values impact the reheating temperature and thus the gravitino abundance, causing  $Y_{3/2}$  to decrease away from the observed bound of  $n_s$ .

In fact, lower equation of state values tend to fall outside the  $n_s$  bound faster than higher values of  $\omega$ . Consequently, this plot underscores the need to reconcile reheating scenarios with observational constraints on gravitino abundance.

## V. GRAVITATIONAL WAVES BACKGROUND

### A. Scalar induced gravitational waves

Detecting the background of primordial gravitational waves would provide strong evidence for the inflation paradigm and offer insights into the fundamental physics of the early Universe [45]. Recent studies have focused on Primordial Gravitational Waves (PGW) from the period immediately following inflation [58–69]. Within the inflationary scenario, the presence of a kinetic epoch preceding inflation leads to a distinct blue tilt in the spectra of primordial gravitational waves at higher frequencies [70]. Gravitational waves are identified as the transverse-traceless component of metric perturbations. According to linear perturbation theory, scalar, vector, and tensor modes do not interact. Now, let us calculate the gravitational waves generated by second-order gravitational interactions resulting from first-order curvature perturbations [71–74]. Using the Newtonian gauge, the perturbed metric is expressed as [75]:

$$ds^2 = a^2(\tau) \left[ -(1 + 2\Phi) d\tau^2 + \left( \delta_{ij} (1 - 2\Phi) + \frac{h_{ij}}{2} \right) dx^i dx^j \right], \quad (5.1)$$

where  $\tau$  is the conformal time,  $\Phi$  represents the first-order Bardeen gravitational potential, and  $h_{ij}$  denotes the second-order tensor perturbation. We can reformulate the spectral abundance of gravitational waves, defined as the energy density of gravitational waves per logarithmic comoving scale, as [76, 77],

$$\Omega_{GW}(k) = \frac{k^2}{12H_0} \mathcal{T}(\tau_0, \mathbf{k}) \mathcal{P}_t(k). \quad (5.2)$$

The time evolution of a gravitational wave field, denoted as  $h_{\mathbf{k}}(\tau_i)$  at an initial conformal time  $\tau_i$  and characterized by its tensor spectrum, can be determined by computing the GW transfer function  $\mathcal{T}(\tau, \mathbf{k}) = h_{\mathbf{k}}(\tau)/h_{\mathbf{k}}(\tau_i)$  [78]. Here,  $h_{\mathbf{k}}(\tau)$  is evaluated at a conformal time  $\eta \gg \eta_i$  [79, 80]. The current conformal time is denoted by  $\tau_0$ , and the Hubble constant is represented by  $H_0$  [85]. Our focus is on the spectral energy density parameter  $\Omega_{GW}(k)$  at Pulsar Timing Array (PTA) scales, where  $f \sim \mathcal{O}(10 - 9) Hz$  corresponds to wavenumbers  $k \sim \mathcal{O}(10^6) Mpc^{-1}$  which are significantly larger than the wavenumber linked to a mode crossing the horizon at matter-radiation equality. Stated differently, the modes observed at PTA scales crossed the horizon deep within the radiation era, well before matter-radiation equality. In the regime where  $k \gg k_{eq}$ , the gravitational wave spectral energy density associated with PTA signals can be expressed as [86–91]

$$\Omega_{GW}(f) = \frac{2\pi^2 f_{yr}^2}{3H_0^2} A^2 \left( \frac{f}{f_{yr}} \right)^\alpha. \quad (5.3)$$

The NANOGrav measurements [92, 93], estimate ranges of several parameters which are given as follows,  $\alpha = (5 - \gamma)$  with  $\gamma = 13/3$ ,  $f_{yr}$  is best estimated to  $f_{yr} \simeq 3.1 \times 10^{-8}$  and  $H_0$  is given by  $H_0 \equiv 100h \text{ km/s/Mpc}$ . The relationship linking the amplitude of the Pulsar Timing Array (PTA) signal, with the cosmological parameters were found to be [94, 95]

$$A = \sqrt{\frac{45\Omega_m^2 A_s}{32\pi^2 (\eta_0 k_{eq})^2}} c \frac{f_{yr}}{\eta_0} \left( \frac{f_{yr}^{-1}}{f_\star} \right)^{\frac{n_T}{2}} \sqrt{r}. \quad (5.4)$$

The dependence on  $n_T$  in this context arises from the substantial "lever arm" between the Cosmic Microwave Background (CMB) pivot frequency, where  $A_s$  is constrained, and the frequency of the Pulsar Timing Array (PTA) signal [ $1yr^{-1}$ ].

Table I presents the NanoGrav proposed model for the density  $h^2\Omega_{gw}(f)$  as a function of frequency  $f$ , scalar-to-tensor ratio  $r$ , and the amplitude of the PTA signal related to the potential parameters of the D-term hybrid model. The model for  $\Omega_{gw}(f)$  depends on various cosmological parameters and constants defined earlier. The analytical expression for,  $h^2\Omega_{gw}(f)$  is derived from a recent theoretical model for primordial gravitational waves.  $h^2\Omega_{gw}(f)$  represents the fractional energy density of gravitational waves in the universe, indicating the energy carried by the gravitational wave background relative to the critical energy density needed for a flat universe. By examining the table

$g$	$\sigma$	$r$	$A$	$f(Hz)$	$h^2\Omega_{gw}(f)$
$3 \times 10^{-3}$	$2 \times 10^{-5}$	0.001	$1.44 \times 10^{-15}$	$4 \times 10^{-8}$	$2.91 \times 10^{-9}$
$2 \times 10^{-3}$	$3 \times 10^{-6}$	0.009	$4.33 \times 10^{-15}$	$2 \times 10^{-8}$	$1.85 \times 10^{-8}$
$4 \times 10^{-3}$	$7 \times 10^{-6}$	0.026	$9.38 \times 10^{-15}$	$1 \times 10^{-8}$	$3.78 \times 10^{-8}$
$5 \times 10^{-3}$	$9 \times 10^{-6}$	0.039	$1.03 \times 10^{-14}$	$8 \times 10^{-7}$	$5.07 \times 10^{-7}$
$4 \times 10^{-3}$	$5 \times 10^{-6}$	0.052	$1.04 \times 10^{-14}$	$6 \times 10^{-7}$	$5.86 \times 10^{-7}$
$5 \times 10^{-3}$	$5 \times 10^{-6}$	0.128	$1.63 \times 10^{-14}$	$4 \times 10^{-7}$	$1.17 \times 10^{-6}$

TABLE I. Testing the density of gravitational waves predicted by PTA as functions of several parameters related to the D-term hybrid model. Here, we have incorporated the best-fit values for the cosmological parameters according to the Planck results [57],  $\Omega_m = 0.315$ ,  $\eta_0 \simeq 1.38$ ,  $A_s = 2, 1 \times 10^{-9}$ ,  $k_{eq} \simeq 0.01$ ,  $f_* \approx 7.7 \times 10^{-17} Hz$ ,  $f_{yr} \simeq 3.1 \times 10^{-8} Hz$  and  $H_0 \equiv 100 h km/s/Mpc$ .

I, one can identify the parameters that predict higher or lower densities of gravitational waves  $h^2\Omega_{gw}(f)$  in line with NANOGrav predictions [81–84]. The amplitude of PTA scales  $A \lesssim 10^{-20}$  provides accurate predictions for  $h^2\Omega_{gw}(f)$  values. Furthermore, the Table I offers insights into the behavior of gravitational wave background (GWB) density concerning frequency, scalar-to-tensor ratio, and the D-term model parameters, demonstrating good consistency with predicted bounds on density and frequency when fine-tuning the inflationary parameters associated with PTA signals.

### B. Primordial Gravitational Waves

For primordial gravitational waves in a spatially flat FLRW background, the metric element can be expressed as follows:

$$ds^2 = a^2(\tau) [-d\tau^2 + (\delta_{ij} + h_{ij}) dx^i dx^j]. \quad (5.5)$$

The perturbation  $h_{ij}$  satisfies the transverse-traceless (TT) conditions:  $h^i_i = 0$  and  $\partial^i h_{ij} = 0$ . The tensor perturbation  $h_{ij}(\tau, \vec{x})$  can be decomposed into its Fourier modes, which are associated with two polarization tensors, satisfying the equation of motion

$$h_{\mathbf{k}}^{\lambda\prime\prime}(\tau) + 2\mathcal{H}h_{\mathbf{k}}^{\lambda\prime}(\tau) + k^2 h_{\mathbf{k}}^{\lambda}(\tau) = 0. \quad (5.6)$$

Here ( $\prime$ ) denotes the derivative with respect to conformal time  $\tau$ , where  $d\tau = \frac{dt}{a}$  and  $\mathcal{H} = \frac{a'}{a}$ . The normalized gravitational wave energy density spectrum is defined as the energy density per logarithmic frequency interval

$$\Omega_{gw}(k) = \frac{1}{\rho_c} \frac{d\rho_{gw}}{d \ln k}, \quad (5.7)$$

here  $\rho_c$  represents the energy density. Additionally,

$$\Omega_{gw,0}(k) = \frac{1}{12} \left( \frac{k^2}{a_0^2 H_0^2} \right) \mathcal{P}_h(k), \quad (5.8)$$

knowing that  $\mathcal{P}_h(k) \equiv \frac{k^3}{\pi^2} \sum_{\lambda} |h_{\mathbf{k}}^{\lambda}|^2$ . By considering the scale at which horizon re-entry occurs ( $k = a_{hc} H_{hc}$ ) and analyzing the horizon re-entry scale alongside the Hubble parameter across different epochs, we can derive the present-day primordial gravitational wave spectrum for mode re-entry during the matter-dominated ( $M$ ), radiation-dominated ( $R$ ), and kinetic ( $K$ ) eras, respectively, as follows:

$$\Omega_{gw,0}^{(M)} = \frac{1}{24} \Omega_{m,0}^2 \frac{a_0^2 H_0^2}{k^2} \mathcal{P}_t \quad (k_0 < k \leq k_{eq}), \quad (5.9)$$

$$\Omega_{gw,0}^{(R)} = \frac{1}{24} \Omega_{r,0}^2 \left( \frac{g_*}{g_{*0}} \right) \left( \frac{g_{*s}}{g_{*s0}} \right) \mathcal{P}_t \quad (k_{eq} < k \leq k_r), \quad (5.10)$$

$$\Omega_{gw,0}^{(K)} = \Omega_{gw,0}^{(R)} \left( \frac{k}{k_r} \right) \quad (k_r < k \leq k_{\max}), \quad (5.11)$$

Fig. 2 provides a detailed visualization of the primordial tensor power spectrum and the corresponding energy density parameters  $\Omega_{gw,0}$  across different cosmological eras: matter-dominated, radiation-dominated, and kinetic eras. In



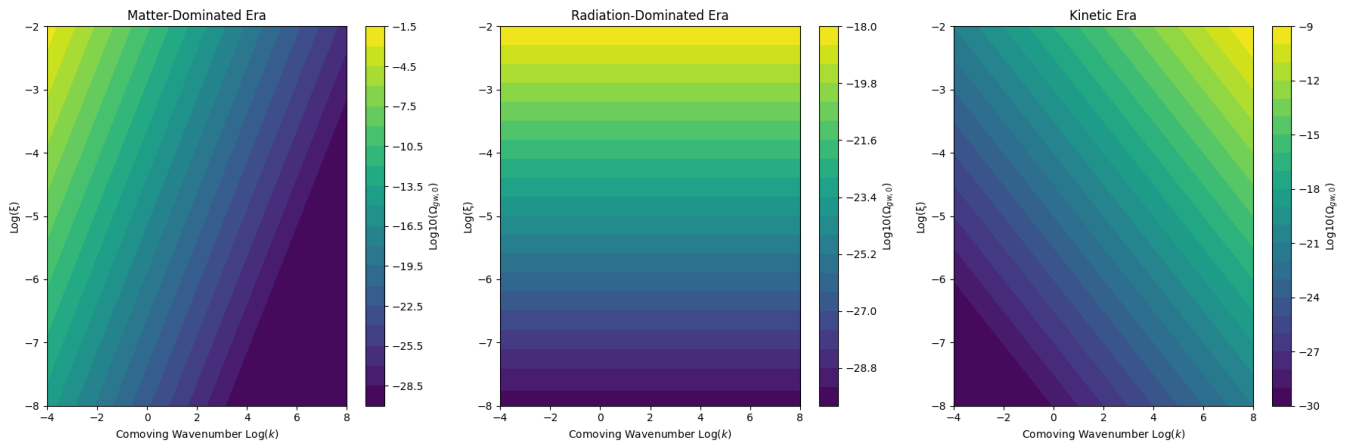


FIG. 2. D-term  $\xi$  parameter as a function of the comoving wavenumber  $k$  across the primordial gravitational wave spectrum  $\Omega_{gw,0}$ .

the matter-dominated era,  $\Omega_{gw,0}$  decreases with increasing comoving wavenumber  $k$ , indicating larger scales are more influenced by primordial tensor perturbations. During the radiation-dominated era, the energy density of gravitational waves is only affected directly by the D-term hybrid parameter  $\xi$ , while the scale  $k$  has a constant effect on  $\Omega_{gw,0}$ . In the kinetic era, the energy density of gravitational waves is increasing with respect to the comoving scale to reach its maximum values at superhorizon scales. This comprehensive depiction illustrates how primordial gravitational waves evolve through different epochs, influenced by the universe's thermal history and expansion dynamics, and underscores the significance of these factors on the energy densities observed.

## VI. CONSTRAINTS ON GRAVITATIONAL WAVES FROM COSMIC STRINGS

Cosmic strings form at the end of inflation, impacting the anisotropies observed in CMB and contributing to the creation of stochastic gravitational waves [100]. The dimensionless string tension,  $G\mu_{cs}$ , is key to understanding these phenomena, where  $G = \frac{1}{8\pi M_p^2} = 6.7 \times 10^{-39} GeV^{-2}$ , and  $\mu_{cs}$  is the string's mass per unit length. Current CMB constraints place limits on this tension as  $G\mu_{cs} \lesssim 1.3 \times 10^{-7}$  [100]. The SGWB arises from a mix of sources including inflation, cosmic strings, and phase transitions [101]. Specifically, inflationary tensor perturbations re-entering the horizon generate an SGWB [102–105], leaving a unique imprint on the CMB B-mode polarization. The amplitude and scale dependence of this background are described by the tensor-to-scalar ratio  $r$  and the tensor spectral index  $n_T$ , adhering to the inflationary consistency relation  $r = -8n_T$  [106]. Given that  $r \geq 0$ , this implies  $n_T \leq 0$  indicating a red spectrum [107]. With current limits on the tensor-to-scalar ratio, the amplitude of the inflationary SGWB at pulsar timing array (PTA) and interferometer scales remains too low for detection by these instruments, necessitating a primordial tensor power spectrum with a strong blue tilt ( $n_T \geq 0$ ) for detection [108, 109].

The detection of gravitational waves from cosmic strings is primarily influenced by two key scales: the energy scale of inflation  $\Lambda_{\text{inf}}$  and the scale at which cosmic strings generate the GW spectrum  $\Lambda_{cs} \equiv \sqrt{G\mu_{cs}}$ . The amplitude of the tensor mode anisotropy in the cosmic microwave background fixes the energy scale of inflation to approximately  $\Lambda_{\text{inf}} \sim V^{1/4} \sim 3.3 \times 10^{16} r^{1/4}$  [110]. By applying the Planck  $2\sigma$  bounds on the tensor-to-scalar ratio  $r$ , we derive an upper limit on the inflation scale,  $\Lambda_{\text{inf}} < 1.6 \times 10^{16} GeV$  [111]. In our model, cosmic strings form post-inflation, indicating  $\Lambda_{\text{inf}} > \Lambda_{cs}$ , which results in a SGWB generated from undiluted strings. The SGWB from metastable cosmic string networks is expressed relative to the critical density as described in the following form [112],

$$\begin{aligned} \Omega_{GW}(f) &= \frac{8\pi G}{3H_0^2} f (G\mu_{cs})^2 \sum_{n=1}^{\infty} C_n(f) P_n, \\ &= \frac{8\pi G}{3H_0^2} f \mathcal{G}_{cs}(C_n, P_n). \end{aligned} \quad (6.1)$$

Here,  $\mathcal{G}_{cs}(C_n, P_n)$  represent the term of cosmic strings contribution to GWs production, which contain the power spectrum  $P_n \simeq \frac{50}{\zeta(4/3)n^{4/3}}$  that represent the gravitational waves (GWs) emitted by the  $n$ -th harmonic of a cosmic string loop, and  $C_n$  which denotes the number of loops emitting GWs observed at a specific frequency  $f$ . The number

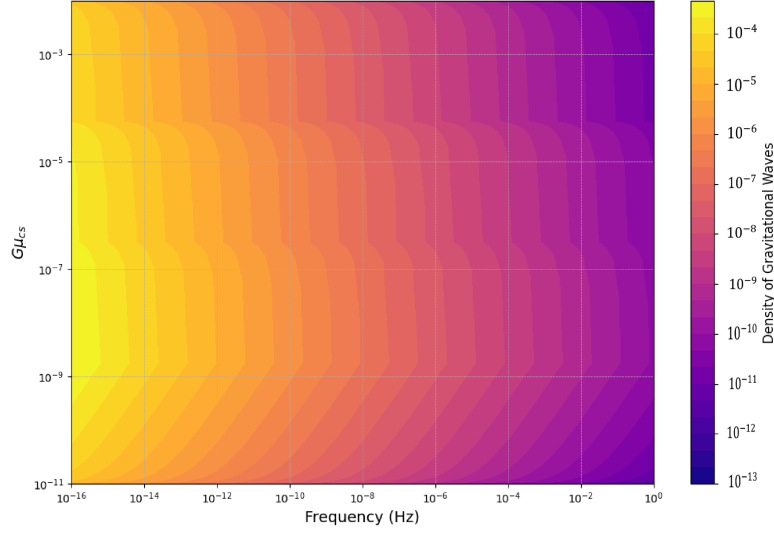


FIG. 3. Gravitational waves density  $\Omega_{GW}$  as a function of the frequency  $f$  and the cosmic string parameter  $G\mu_{cs}$ .

of loops emitting GWs, observed at a given frequency  $f$  is defined as [112],

$$C_n(f) = \frac{2n}{f^2} \int_{z_{\min}}^{z_{\max}} \frac{dz}{H(z)(1+z)^6} \mathcal{N}(l, t). \quad (6.2)$$

The integration range spans the lifetime of the cosmic string network, starting from its formation at  $z_{\max} \simeq \frac{T_R}{2.7K}$ , with  $T_R$  being approximately  $10^9 GeV$  to its decay at  $z_{\min} = \left(\frac{70}{H_0}\right)^{1/2} \left(\frac{\Gamma(G\mu_{cs})^2}{2\pi \times 6.7 \times 10^{-39}} \exp(-\pi\kappa_{cs})\right)^{1/4}$  [113], where  $\Gamma \simeq 50$  is a numerical factor specifying the cosmic strings decay rate. Here,  $\mathcal{N}(l, t)$  represents the number density of CS loops of length  $l = \frac{2n}{(1+z)f}$ . The loop density is defined by considering their formation and decay across different epochs. For the region of interest, the dominant contribution arises from the loops generated during the radiation-dominated era which is given by [113],

$$\mathcal{N}_r(l, t) = \frac{0.18}{t^{2/3} (l + \Gamma G\mu_{cs} t)^{5/2}}. \quad (6.3)$$

The cosmological time and the Hubble rate with the current values of matter, radiation and dark energy densities, are respectively expressed as a function of the redshift  $z$  as  $t(z) = \int_{z_{\min}}^{z_{\max}} \frac{dz}{H(z)(1+z)}$ ,  $H(z) = H_0 \sqrt{\Omega_\Lambda + \Omega_m (1+z)^3 + \Omega_r (1+z)^4}$ .

Fig. 3 illustrates the density of gravitational waves  $\Omega_{GW}$  as a function of frequency  $f$  and the cosmic string parameter  $G\mu_{cs}$ . The contour plot uses a logarithmic scale for both the frequency and  $G\mu_{cs}$ , highlighting how gravitational wave densities vary across different scales and parameters. The gravitational wave energy density is computed by integrating over the redshift  $z$ , taking into account the contributions from matter, radiation, and dark energy to the Hubble parameter  $H(z)$ . The function  $\mathcal{N}_r(l, t)$  reflects the number density of gravitational waves, which is influenced by the redshift and other cosmological parameters.  $C_n$  and  $P_n$  are functions of  $n$ , frequency  $f$ , and the cosmic string parameter  $G\mu_{cs}$ , representing cosmic strings contribution to the power spectrum of the gravitational waves. The resulting plot shows that at higher frequencies, the gravitational wave density varies more significantly with changes in  $G\mu_{cs}$ , indicating a strong dependence on the string tension parameter. This comprehensive depiction underscores the intricate relationship between cosmic string dynamics and gravitational wave emissions, offering insights into how different frequencies and cosmic string tensions contribute to the observable gravitational wave background. The use of a logarithmic scale for both axes ensures that a wide range of values is represented, making it easier to visualize the detailed structure and variation of  $\Omega_{GW}$  across different cosmological scenarios.

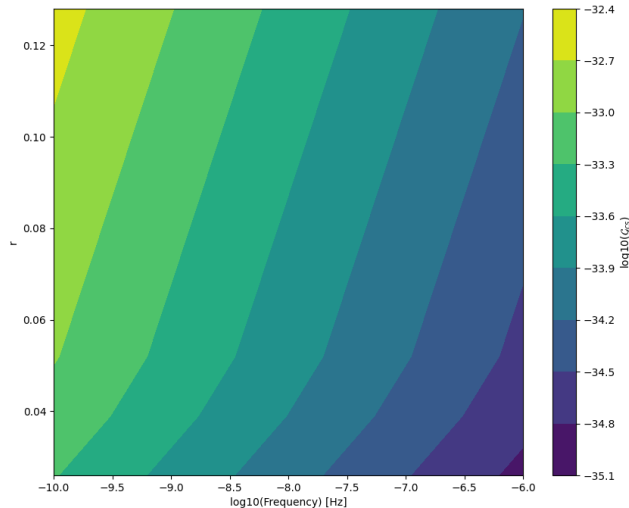


FIG. 4. Cosmic strings factor  $\mathcal{G}_{cs}$  as functions of the frequency  $f$  and the tensor-to-scalar ratio  $r$ .

Fig. 4 presents the cosmic strings factor  $\mathcal{G}_{cs}$  as a function of frequency and the tensor-to-scalar ratio  $r$ . The contour plot uses a logarithmic scale for frequency, ranging from  $10^{-10} Hz$  to  $10^{-6} Hz$ , and spans multiple values of  $r = [0.026, 0.128]$ , reflecting different possible strengths of primordial tensor perturbations. The frequency dependence of  $\mathcal{G}_{cs}$  incorporates a power-law behavior with an exponent  $\alpha$ , representing the spectral shape of the cosmic string signal. The resulting plot visually demonstrates that  $\mathcal{G}_{cs}$  increases with higher values of  $r$  and decreases with increasing frequency. The contour levels indicate the logarithmic values of, with color gradients representing the intensity. This visualization helps to elucidate the relationship between cosmic string dynamics and gravitational wave signals across a range of frequencies and tensor-to-scalar ratios. Specifically, it shows that stronger primordial tensor perturbations lead to higher  $\mathcal{G}_{cs}$  values, particularly at lower frequencies, which is crucial for understanding the potential observational signatures of cosmic strings in gravitational wave experiments. This comprehensive depiction provides insights into the scale and strength of cosmic string contributions to the gravitational wave background, highlighting key dependencies and aiding in the interpretation of potential observational data in the context of early universe cosmology.

## VII. CONCLUSION

In this paper, we investigated the framework of supergravity model, employing the minimal Kähler potential. Our study revealed that D-term potential can circumvent the  $\eta$ -problem inherent in F-term models, offering a viable path to successful inflation. Mathematically, we derived the scalar potential, incorporating both F-term and D-term contributions, and demonstrated the stability conditions for the inflaton field  $S$ . The effective potential during inflation was approximated, highlighting the importance of the gauge coupling constant  $g$  and the Fayet-Iliopoulos term  $\xi$ . The slow-roll parameters and the resulting e-folding number were calculated, providing insights into the inflationary dynamics. Furthermore, we explored reheating dynamics and gravitino production, emphasizing the interplay between reheating temperature  $T_{re}$ , spectral index  $n_s$ , and gravitino abundance  $Y_{3/2}$ . Our analysis indicated that gravitino production is sensitive to the equation of state during reheating, impacting the reheating temperature and the subsequent dark matter relic density.

The study of scalar induced gravitational waves offers crucial insights into the early Universe, particularly within the inflationary paradigm. Detecting the primordial gravitational wave background can substantiate inflationary models by providing evidence for a kinetic epoch preceding inflation, characterized by a distinct blue tilt at higher frequencies. The perturbation theory framework reveals that the transverse-traceless components of these waves evolve according to second-order gravitational interactions induced by first-order curvature perturbations. The spectral energy density of these waves at various scales, particularly those relevant to Pulsar Timing Array (PTA) observations, can be quantified through analytical models, which align well with empirical data, such as that from NANOGrav. These

models illustrate the dependence of gravitational wave amplitudes on key cosmological parameters, thus highlighting the interplay between inflationary dynamics and observable gravitational wave spectra.

The analysis of gravitational waves generated by cosmic strings provides critical constraints on the dynamics of the early Universe and the properties of cosmic strings. The dimensionless string tension,  $G\mu_{cs}$ , significantly influences the stochastic gravitational wave background (SGWB) produced by cosmic strings post-inflation. Current constraints from CMB observations limit  $G\mu_{cs} \leq 1.3 \times 10^{-7}$ . The SGWB from cosmic strings is shaped by the energy scales of inflation and the string formation, with the amplitude of tensor mode anisotropy fixing the inflation scale around  $\Lambda_{\text{inf}} \sim 3.3 \times 10^{16} r^{1/4}$ . Cosmic string contributions to the gravitational wave spectrum, represented by  $\Omega_{GW}(f)$ , depend on the number density and dynamics of cosmic string loops across different cosmological epochs. These contributions exhibit a strong frequency dependence and vary significantly with the string tension parameter, highlighting the complex relationship between cosmic string properties and observable gravitational wave signals. The comprehensive models and visualizations underscore the importance of cosmic string dynamics in shaping the SGWB and provide insights into potential observational signatures in gravitational wave experiments, aiding in the broader understanding of early universe cosmology.

### ACKNOWLEDGMENTS

G.O. acknowledges the financial support of Fondecyt Grant 1220065.

- 
- [1] Dvali, G., Shafi, Q., & Schaefer, R. (1994). *Large scale structure and supersymmetric inflation without fine tuning*. Physical Review Letters, 73(14), 1886.
  - [2] Copeland, E. J., Liddle, A. R., Lyth, D. H., Stewart, E. D., & Wands, D. (1994). *False vacuum inflation with Einstein gravity*. Physical Review D, 49(12), 6410.
  - [3] Linde, A., & Riotto, A. (1997). *Hybrid inflation in supergravity*. Physical Review D, 56(4), R1841.
  - [4] Şenoğuz, V. N., & Shafi, Q. (2005). *Reheat temperature in supersymmetric hybrid inflation models*. Physical Review D, 71(4), 043514.
  - [5] Senoguz, V. N., & Shafi, Q. (2003). *Testing supersymmetric grand unified models of inflation*. Physics Letters B, 567(1-2), 79-86.
  - [6] Rehman, M. U., Shafi, Q., & Wickman, J. R. (2010). *Supersymmetric hybrid inflation redux*. Physics Letters B, 683(2-3), 191-195.
  - [7] Afzal, A., Ahmed, W., Rehman, M. U., & Shafi, Q. (2022).  *$\mu$ -hybrid inflation, gravitino dark matter, and stochastic gravitational wave background from cosmic strings*. Physical Review D, 105(10), 103539.
  - [8] McDonald, J. (2004). *Conditions for a successful right-handed Majorana sneutrino curvaton*. Physical Review D, 70(6), 063520.
  - [9] Copeland, E. J., Liddle, A. R., Lyth, D. H., Stewart, E. D., & Wands, D. (1994). *False vacuum inflation with Einstein gravity*. Physical Review D, 49(12), 6410.
  - [10] Seto, O., & Yokoyama, J. I. (2006). *Hiding cosmic strings in supergravity D-term inflation*. Physical Review D, 73(2), 023508.
  - [11] Halyo, E. (1996). *Hybrid inflation from supergravity D-terms*. Physics Letters B, 387(1), 43-47.
  - [12] Binetruy, P., & Dvali, G. (1996). *D-term inflation*. Physics Letters B, 388(2), 241-246.
  - [13] Lyth, D. H., & Riotto, A. (1999). Particle physics models of inflation and the cosmological density perturbation. Physics Reports, 314(1-2), 1-146.
  - [14] Jeannerot, R. (1997). Inflation in supersymmetric unified theories. Physical Review D, 56(10), 6205.
  - [15] Linde, A. (1994). *Hybrid inflation*. Physical Review D, 49(2), 748.
  - [16] King, S. F., & Riotto, A. (1998). *Dilaton stabilisation in D-term inflation*. Physics Letters B, 442(1-4), 68-73.
  - [17] Ellis, J., Kim, J. E., & Nanopoulos, D. V. (1984). *Cosmological gravitino regeneration and decay*. Physics Letters B, 145(3-4), 181-186.
  - [18] Ellis, J., Nanopoulos, D. V., Olive, K. A., & Rey, S. J. (1996). *On the thermal regeneration rate for light gravitinos in the early universe*. Astroparticle Physics, 4(4), 371-385.
  - [19] Giudice, G. F., Riotto, A., & Tkachev, I. (1999). *Thermal and non-thermal production of gravitinos in the early universe*. Journal of High Energy Physics, 1999(11), 036.
  - [20] Ellis, J., Linde, A. D., Nanopoulos, D. V. (1982). *Inflation can save the gravitino*. Physics Letters B, 118(1-3), 59-64.
  - [21] King, S. F., Pascoli, S., Turner, J., & Zhou, Y. L. (2021). *Gravitational waves and proton decay: complementary windows into grand unified theories*. Physical Review Letters, 126(2), 021802.
  - [22] Buchmuller, W., Domcke, V., & Schmitz, K. (2020). *From NANOGrav to LIGO with metastable cosmic strings*. Physics Letters B, 811, 135914.

- [23] King, S. F., Pascoli, S., Turner, J., & Zhou, Y. L. (2021). *Confronting SO (10) GUTs with proton decay and gravitational waves*. Journal of High Energy Physics, 2021(10), 1-38.
- [24] Benetti, M., Graef, L. L., & Vagnozzi, S. (2022). *Primordial gravitational waves from NANOGrav: A broken power-law approach*. Physical Review D, 105(4), 043520.
- [25] Ahriche, A., Hashino, K., Kanemura, S., & Nasri, S. (2019). *Gravitational waves from phase transitions in models with charged singlets*. Physics Letters B, 789, 119-126.
- [26] Scientific, L. I. G. O., Abbott, B. P., Abbott, R., Abbott, T. D., Abraham, S., Acernese, F., ... & Calloni, E. (2019). *Search for the isotropic stochastic background using data from Advanced LIGO's second observing run*. Physical Review D, 100(6), 061101.
- [27] Amaro-Seoane, P., Audley, H., Babak, S., Baker, J., Barausse, E., Bender, P., ... & Zweifel, P. (2017). *Laser interferometer space antenna*. arXiv preprint arXiv:1702.00786.
- [28] Goncharov, B., Shannon, R. M., Reardon, D. J., Hobbs, G., Zic, A., Bailes, M., ... & Zhang, S. (2021). *On the evidence for a common-spectrum process in the search for the nanohertz gravitational-wave background with the Parkes Pulsar Timing Array*. The Astrophysical Journal Letters, 917(2), L19.
- [29] Wess, J., & Bagger, J. (1992). *Supersymmetry and supergravity (Vol. 103)*. Princeton university press.
- [30] Nilles, H. P. (1984). *Supersymmetry, supergravity and particle physics*. Physics Reports, 110(1-2), 1-162.
- [31] Bailin, D., & Love, A. (1994). *Supersymmetric gauge field theory and string theory (p. 322)*. Taylor & Francis.
- [32] YAMAGUCHI, Masahide. *Supergravity-based inflation models: a review*. Classical and Quantum Gravity, 2011, vol. 28, no 10, p. 103001.
- [33] Stewart, E. D. (1995). *Inflation, supergravity, and superstrings*. Physical Review D, 51(12), 6847.
- [34] Binétruy, P., & Dvali, G. (1996). *D-term inflation*. Physics Letters B, 388(2), 241-246.
- [35] Halyo, E. (1996). *Hybrid inflation from supergravity D-terms*. Physics Letters B, 387(1), 43-47.
- [36] Coleman, S., & Weinberg, E. (1973). *Radiative corrections as the origin of spontaneous symmetry breaking*. Physical Review D, 7(6), 1888.
- [37] BARDEEN, James M. *Gauge-invariant cosmological perturbations*. Physical Review D, 1980, vol. 22, no 8, p. 1882.
- [38] M. Gonzalez-Espinoza, G. Otalora, N. Videla and J. Saavedra, JCAP **08** (2019), 029
- [39] M. Gonzalez-Espinoza and G. Otalora, Phys. Lett. B **809** (2020), 135696
- [40] Y. Leyva, C. Leiva, G. Otalora and J. Saavedra, Phys. Rev. D **105** (2022) no.4, 043523
- [41] Y. Leyva and G. Otalora, JCAP **04** (2023), 030
- [42] HAWKING, Stephen W. *The development of irregularities in a single bubble inflationary universe*. Physics Letters B, 1982, vol. 115, no 4, p. 295-297.
- [43] STAROBINSKY, Alexei A. *Dynamics of phase transition in the new inflationary universe scenario and generation of perturbations*. Physics Letters B, 1982, vol. 117, no 3-4, p. 175-178.
- [44] Mansfield, G., Fan, J., Lu, Q. (2023). *Phenomenology of Spillway Preheating: Equation of State and Gravitational Waves*. arXiv preprint arXiv:2312.03072.
- [45] Ade, P. A. R., Desert, F. X., Knoche, J., Giard, M., Dupac, X., Liguori, M., ... Hernandez-Monteagudo, C. (2015). *Planck 2015. XX. Constraints on inflation*. Astron. Astrophys., 594(arXiv: 1502.02114), A20.
- [46] GUTH, Alan H. et PI, So-Young. *Fluctuations in the new inflationary universe*. Physical Review Letters, 1982, vol. 49, no 15, p. 1110.
- [47] STAROBINSKY, Alexei A. *Relict gravitation radiation spectrum and initial state of the universe*. JETP lett, 1979, vol. 30, no 682-685, p. 131-132.
- [48] DAI, Liang, KAMIONKOWSKI, Marc, et WANG, Junpu. *Reheating constraints to inflationary models*. Physical review letters, 2014, vol. 113, no 4, p. 041302.
- [49] COOK, Jessica L., DIMASTROGIOVANNI, Emanuela, EASSON, Damien A., et al. *Reheating predictions in single field inflation*. Journal of Cosmology and Astroparticle Physics, 2015, vol. 2015, no 04, p. 047.
- [50] M. López, G. Otalora and N. Videla, JCAP **10** (2021), 021
- [51] DINE, Michael, KITANO, Ryuichiro, MORISSE, Alexander, et al. *Moduli decays and gravitinos*. Physical Review D, 2006, vol. 73, no 12, p. 123518.
- [52] ENDO, Motoi, HAMAGUCHI, Koichi, et TAKAHASHI, Fuminobu. *Moduli/inflaton mixing with supersymmetry-breaking field*. Physical Review D, 2006, vol. 74, no 2, p. 023531.
- [53] Endo, M., Kawasaki, M., Takahashi, F., & Yanagida, T. T. (2006). *Inflaton decay through supergravity effects*. Physics Letters B, 642(5-6), 518-524.
- [54] TAKAHASHI, Fuminobu. *Inflaton decay in supergravity and gravitino problem*. In : AIP Conference Proceedings. American Institute of Physics, 2008. p. 57-60.
- [55] ENDO, Motoi, TAKAHASHI, Fuminobu, et YANAGIDA, T. T. *Inflaton decay in supergravity*. Physical Review D, 2007, vol. 76, no 8, p. 083509.
- [56] NAKAYAMA, Kazunori, TAKAHASHI, Fuminobu, et YANAGIDA, Tsutomu T. *Constraint on the gravitino mass in hybrid inflation*. Journal of Cosmology and Astroparticle Physics, 2010, vol. 2010, no 12, p. 010.
- [57] P. Collaboration, N. Aghanim, Y. Akrami, M. Ashdown, J. Aumont, C. Baccigalupi, et al. (2020). *Planck 2018 results. VI. Cosmological parameters*
- [58] Easther, R., Lim, E. A. (2006). *Stochastic gravitational wave production after inflation*. Journal of Cosmology and Astroparticle Physics, 2006(04), 010.
- [59] An, H., Yang, C. (2024). *Gravitational waves produced by domain walls during inflation*. Physical Review D, 109(12), 123508.

- [60] Eggemeier, B., Niemeyer, J. C., Jedamzik, K., Easther, R. (2023). *Stochastic gravitational waves from postinflationary structure formation*. Physical Review D, 107(4), 043503.
- [61] El Bourakadi, K., Ferricha-Alami, M., Filali, H., Sakhi, Z., & Bennai, M. (2021). *Gravitational waves from preheating in Gauss–Bonnet inflation*. The European Physical Journal C, 81(12), 1144.
- [62] El Bourakadi, K., Asfour, B., Sakhi, Z., Bennai, M., & Ouali, T. (2022). *Primordial black holes and gravitational waves in teleparallel Gravity*. The European Physical Journal C, 82(9), 792.
- [63] El Bourakadi, K., Bousder, M., Sakhi, Z., & Bennai, M. (2021). *Preheating and reheating constraints in supersymmetric braneworld inflation*. The European Physical Journal Plus, 136(8), 1-19.
- [64] Sakhi, Z., El Bourakadi, K., Safsafi, A., Ferricha-Alami, M., Chakir, H., & Bennai, M. (2020). *Effect of brane tension on reheating parameters in small field inflation according to Planck-2018 data*. International Journal of Modern Physics A, 35(30), 2050191.
- [65] Bousder, M., El Bourakadi, K., & Bennai, M. (2021). *Charged 4d einstein-gauss-bonnet black hole: Vacuum solutions, cauchy horizon, thermodynamics*. Physics of the Dark Universe, 32, 100839.
- [66] El Bourakadi, K., Sakhi, Z., & Bennai, M. (2022). *Preheating constraints in  $\alpha$ -attractor inflation and Gravitational Waves production*. International Journal of Modern Physics A, 37(17), 2250117.
- [67] El Bourakadi, K., Koussour, M., Otalora, G., Bennai, M., & Ouali, T. (2023). *Constant-roll and primordial black holes in  $f(Q, T)$  gravity*. Physics of the Dark Universe, 41, 101246.
- [68] El Bourakadi, K., Ferricha-Alami, M., Sakhi, Z., Bennai, M., & Chakir, H. (2024). *Dark matter via baryogenesis: Affleck–Dine mechanism in the minimal supersymmetric standard model*. Modern Physics Letters A, 2450060.
- [69] Bourakadi, K. E., Chakir, H., Khlopov, M. Y. (2024). *Leptogenesis Effects on the Gravitational Waves Background: Interpreting the NANOGrav Measurements and JWST Constraints on Primordial Black Holes*. arXiv preprint arXiv:2401.05311.
- [70] Ebadi, R., Kumar, S., McCune, A., Tai, H., Wang, L. T. (2024). *Gravitational waves from stochastic scalar fluctuations*. Physical Review D, 109(8), 083519.
- [71] MATARRESE, Sabino, PANTANO, Ornella, et SAEZ, Diego. *General-relativistic approach to the nonlinear evolution of collisionless matter*. Physical Review D, 1993, vol. 47, no 4, p. 1311.
- [72] MATARRESE, Sabino, PANTANO, Ornella, et SAEZ, Diego. *General relativistic dynamics of irrotational dust: Cosmological implications*. Physical review letters, 1994, vol. 72, no 3, p. 320.
- [73] MCCORMICK, Stephen. *First law of black hole mechanics as a condition for stationarity*. Physical Review D, 2014, vol. 90, no 10, p. 104034.
- [74] DOMENECH, Guillem. *Scalar induced gravitational waves review*. Universe, 2021, vol. 7, no 11, p. 398.
- [75] Basilakos, S., Nanopoulos, D. V., Papanikolaou, T., Saridakis, E. N., & Tzerefos, C. (2024). *Gravitational wave signatures of no-scale Supergravity in NANOGrav and beyond*. Physics Letters B, 138507.
- [76] Kohri, K., & Terada, T. (2018). *Semianalytic calculation of gravitational wave spectrum nonlinearly induced from primordial curvature perturbations*. Physical Review D, 97(12), 123532.
- [77] Maggiore, M. (2000). *Gravitational wave experiments and early universe cosmology*. Physics Reports, 331(6), 283-367.
- [78] Baumann, D., Steinhardt, P., Takahashi, K., & Ichiki, K. (2007). *Gravitational wave spectrum induced by primordial scalar perturbations*. Physical Review D, 76(8), 084019.
- [79] Vagnozzi, S. (2021). *Implications of the NANOGrav results for inflation*. Monthly Notices of the Royal Astronomical Society: Letters, 502(1), L11-L15.
- [80] Zhao, W., Zhang, Y., You, X. P., & Zhu, Z. H. (2013). *Constraints of relic gravitational waves by pulsar timing arrays: Forecasts for the FAST and SKA projects*. Physical Review D, 87(12), 124012.
- [81] Afzal, A., Agazie, G., Anumarpudi, A., Archibald, A. M., Arzoumanian, Z., Baker, P. T., ..., NANOGrav Collaboration. (2023). *The NANOGrav 15 yr data set: search for signals from new physics*. The Astrophysical Journal Letters, 951(1), L11.
- [82] Agazie, G., Anumarpudi, A., Archibald, A. M., Arzoumanian, Z., Baker, P. T., Bécsy, B., ..., NANOGrav Collaboration. (2023). *The NANOGrav 15 yr data set: evidence for a gravitational-wave background*. The Astrophysical Journal Letters, 951(1), L8.
- [83] Agazie, G., Alam, M. F., Anumarpudi, A., Archibald, A. M., Arzoumanian, Z., Baker, P. T., ..., NANOGrav Collaboration. (2023). *The NANOGrav 15 yr data set: Observations and timing of 68 millisecond pulsars*. The Astrophysical Journal Letters, 951(1), L9.
- [84] Wu, Y. M., Chen, Z. C., Huang, Q. G. (2023). *Search for stochastic gravitational-wave background from massive gravity in the NANOGrav 12.5-year dataset*. Physical Review D, 107(4), 042003.
- [85] Kuroyanagi, S., Chiba, T., & Sugiyama, N. (2009). *Precision calculations of the gravitational wave background spectrum from inflation*. Physical Review D, 79(10), 103501.
- [86] Afzal, A., Agazie, G., Anumarpudi, A., Archibald, A. M., Arzoumanian, Z., Baker, P. T., ... & NANOGrav Collaboration. (2023). *The NANOGrav 15 yr Data Set: Search for Signals from New Physics*. The Astrophysical Journal Letters, 951(1), L11.
- [87] Agazie, G., Anumarpudi, A., Archibald, A. M., Arzoumanian, Z., Baker, P. T., Bécsy, B., ... & NANOGrav Collaboration. (2023). *The NANOGrav 15 yr data set: Evidence for a gravitational-wave background*. The Astrophysical Journal Letters, 951(1), L8.
- [88] Agazie, G., Alam, M. F., Anumarpudi, A., Archibald, A. M., Arzoumanian, Z., Baker, P. T., ... & NANOGrav Collaboration. (2023). *The NANOGrav 15 yr Data Set: Observations and Timing of 68 Millisecond Pulsars*. The Astrophysical Journal Letters, 951(1), L9.

- [89] Arzoumanian, Z., Baker, P. T., Blumer, H., Bécsy, B., Brazier, A., Brook, P. R., ... & NANOGrav Collaboration. (2020). *The NANOGrav 12.5 yr data set: search for an isotropic stochastic gravitational-wave background*. The Astrophysical Journal Letters, 905(2), L34.
- [90] Arzoumanian, Z., Brazier, A., Burke-Spolaor, S., Chamberlin, S. J., Chatterjee, S., Christy, B., ... & NANOGrav Collaboration. (2016). *The NANOGrav nine-year data set: limits on the isotropic stochastic gravitational wave background*. The Astrophysical Journal, 821(1), 13.
- [91] Guo, S. Y., Khlopov, M., Liu, X., Wu, L., Wu, Y., & Zhu, B. (2023). *Footprints of Axion-Like Particle in Pulsar Timing Array Data and JWST Observations*. arXiv preprint arXiv:2306.17022.
- [92] Arzoumanian, Z., Baker, P. T., Blumer, H., Bécsy, B., Brazier, A., Brook, P. R., ... & NANOGrav Collaboration., *The NANOGrav 12.5 yr data set: search for an isotropic stochastic gravitational-wave background*. The Astrophysical journal letters 905 (2), L34 (2020).
- [93] Gao, T. J., & Yang, X. Y., *Double peaks of gravitational wave spectrum induced from inflection point inflation*. The European Physical Journal C, 81 (6), 1-10 (2021).
- [94] Vagnozzi, S. (2023). *Inflationary interpretation of the stochastic gravitational wave background signal detected by pulsar timing array experiments*. Journal of High Energy Astrophysics.
- [95] Zhao, W., Zhang, Y., You, X. P., & Zhu, Z. H. (2013). *Constraints of relic gravitational waves by pulsar timing arrays: Forecasts for the FAST and SKA projects*. Physical Review D, 87(12), 124012.
- [96] Sahni, V., Sami, M., & Souradeep, T. (2001). *Relic gravity waves from braneworld inflation*. Physical Review D, 65(2), 023518.
- [97] Figueroa, D. G., & Tanin, E. H. (2019). *Inconsistency of an inflationary sector coupled only to Einstein gravity*. Journal of Cosmology and Astroparticle Physics, 2019(10), 050.
- [98] Giovannini, M. (1998). *Gravitational wave constraints on post-inflationary phases stiffer than radiation*. Physical Review D, 58(8), 083504.
- [99] Riazuelo, A., & Uzan, J. P. (2000). *Quintessence and gravitational waves*. Physical Review D, 62(8), 083506.
- [100] Akrami, Y., Arroja, F., Ashdown, M., Aumont, J., Baccigalupi, C., Ballardini, M., ... & Tomasi, M. (2020). *Planck 2018 results-IX. Constraints on primordial non-Gaussianity*. Astronomy & Astrophysics, 641, A9.
- [101] Aghanim, N., Akrami, Y., Ashdown, M., Aumont, J., Baccigalupi, C., Ballardini, M., ... & Roudier, G. (2020). *Planck 2018 results-VI. Cosmological parameters*. Astronomy & Astrophysics, 641, A6.
- [102] Vagnozzi, S. (2021). *Implications of the NANOGrav results for inflation*. Monthly Notices of the Royal Astronomical Society: Letters, 502(1), L11-L15.
- [103] Benetti, M., Graef, L. L., & Vagnozzi, S. (2022). *Primordial gravitational waves from NANOGrav: A broken power-law approach*. Physical Review D, 105(4), 043520.
- [104] Caprini, C. (2015, April). *Stochastic background of gravitational waves from cosmological sources*. In Journal of Physics: Conference Series (Vol. 610, No. 1, p. 012004). IOP Publishing.
- [105] Kuroyanagi, S., Takahashi, T., & Yokoyama, S. (2021). *Blue-tilted inflationary tensor spectrum and reheating in the light of NANOGrav results*. Journal of Cosmology and Astroparticle Physics, 2021(01), 071.
- [106] Liddle, A. R., & Lyth, D. H. (1993). *The Cold dark matter density perturbation*. Physics Reports, 231(1-2), 1-105.
- [107] Ade, P. A. R., Ahmed, Z., Aikin, R. W., Alexander, K. D., Barkats, D., Benton, S. J., ... & (Keck Array and bicep2 Collaborations). (2018). *Constraints on Primordial Gravitational Waves Using Planck, WMAP, and New BICEP2/Keck Observations through the 2015 Season*. Physical review letters, 121(22), 221301.
- [108] Vagnozzi, S. (2021). *Implications of the NANOGrav results for inflation*. Monthly Notices of the Royal Astronomical Society: Letters, 502(1), L11-L15.
- [109] Ahmed, W., Junaid, M., Nasri, S., & Zubair, U. (2022). *Constraining the cosmic strings gravitational wave spectra in no-scale inflation with viable gravitino dark matter and nonthermal leptogenesis*. Physical Review D, 105(11), 115008.
- [110] Easther, R., Kinney, W. H., & Powell, B. A. (2006). *The Lyth bound and the end of inflation*. Journal of Cosmology and Astroparticle Physics, 2006(08), 004.
- [111] Akrami, Y., Arroja, F., Ashdown, M., Aumont, J., Baccigalupi, C., Ballardini, M., ... & Savelainen, M. (2020). *Planck 2018 results-X. Constraints on inflation*. Astronomy & Astrophysics, 641, A10.
- [112] Blanco-Pillado, J. J., & Olum, K. D. (2017). *Stochastic gravitational wave background from smoothed cosmic string loops*. Physical Review D, 96(10), 104046.
- [113] Buchmuller, W., Domcke, V., & Schmitz, K. (2020). *From NANOGrav to LIGO with metastable cosmic strings*. Physics Letters B, 811, 135914.
- [114] Auclair, P., Blanco-Pillado, J. J., Figueroa, D. G., Jenkins, A. C., Lewicki, M., Sakellariadou, M., ... & Kuroyanagi, S. (2020). *Probing the gravitational wave background from cosmic strings with LISA*. Journal of Cosmology and Astroparticle Physics, 2020(04), 034.